Front. Phys. 10, 108601 (2015)
DOI 10.1007/s11467-014-0440-2

RESEARCH ARTICLE

Molecular dynamics study of the infiltration of lipid-wrapping C_{60} and polyhydroxylated single-walled nanotubes into lipid bilayers

Guan-Xing Guo, Lei Zhang, Yong Zhang†

School of Physics and Engineering, Sun Yat-Sen University, Guangzhou 510275, China

Corresponding author. E-mail: †*zhyong9@mail.sysu.edu.cn*

Received May 8, 2014; accepted July 18, 2014

Because of the many potential medical applications of nanoparticles, considerable research has been conducted on the interactions between nanoparticles and biomembranes. We employed coarse-grained molecular dynamics simulations to study the infiltration of lipid-wrapping C_{60} and polyhydroxylated single-walled nanotubes. Diffusion coefficients and scaling factors are adopted to quantify the diffusivity of the biomembranes, and the rupture tension is used to measure the lateral strength of the lipid bilayer. According to our simulations, all wrapped nanoparticles, except those wrapped by dipalmitoyl-glycero-phosphoglycerol, can be inserted into the bilayers. Our simulations also reveal that the bilayers remain in free diffusion after the nanoparticle insertions while their diffusion coefficient can be altered significantly. The polyhydroxylated single-walled nanotubes lead to significant changes to the lateral strength of biomembranes and this effect depends on the quantity of the inserted nanoparticles. The simulations demonstrate the feasibility of using these methods to deliver nanoparticles while some suggestions are given for choosing the appropriate lipids for wrapping. The results also suggest that the functionalized nanoparticles could be applied in strengthening or weakening the lateral strength of biomembranes for specific purposes.

Keywords lipid bilayer, carbon nanoparticle, molecular dynamics

PACS numbers 86.16.dm, 87.15.ap, 82.70.Uv

1 Introduction

Nanotechnology has been growing fast in the past decade. Nanoparticles with dimensions between 1 and 100 nm have significant effects on living organisms [1–3]. Among them, C_{60} and carbon nanotubes (CNTs) have been studied extensively [4–7]. Their influence on biomembranes has revealed that these nanoparticles have plenty of potential applications in medicine [8–10], particularly for cancer therapy drug delivery [11]. Experiments and simulations have already shown that the small size of the nanoparticles results in their uptake through biomembranes [12, 13]. Studies on C_{60} have shown that C_{60} can infiltrate the membrane and diffuse into the interior [14]. The insertion of these nanoparticles through the lipid bilayer depends on their shape [15]. The effects of C_{60} on the mechanical properties of the biomembranes also depends on their size and shape [16]. However, other research on C_{60} has shown that it alters the mechanical characteristics of human red blood cells and may even cause extensive damage to the cells [17]. Similar phenomena or even worse situations such as asbestos-like pathogenicity may occur if the human cell membranes are exposed to these nanoparticles [18, 19]. Since biomembranes perform significant functions in a living organism, any deleterious effects on the membranes from nanoparticles can result in their dysfunction or even cell damage. Such cytotoxicity has been reported and there might be other potential cytotoxicities, so solutions to this problem require more investigation [20, 21].

Some simulations on single-walled carbon nanotubes (SWNTs) indicate that they can penetrate a lipid bilayer and stay in its center bilayer [22]. The penetrability of SWNTs into biomembranes is usually related to their length and chirality [5]. Further study of nanoparticles entering through biomembranes is required for their application within living organisms in the future.

Applications for drug delivery based on these particles have been developed for specific diseases, although challenges still remain [23, 24]. A means to deliver the nanoparticle evenly inside a cell is necessary. As most carbon nanoparticles including C_{60} are hydrophobic, they tend to aggregate together in a aqueous solution and this property prevents them from distributing evenly within the cells. A solution is to wrap the nanoparticles with a lipid whose head is hydrophilic while its tail is hydrophobic. When the lipids and carbon nanoparticles are put into an aqueous solution, the lipids will aggregate around the nanoparticles and wrap them with their head pointing outward. A single nanoparticle can be wrapped in this way, thereby separating them from each other. Such methods have been adopted in the deliveries of larger particles, such as DNA, in experiments [25]. Research has been performed on some lipid-wrapping nanoparticles for delivery [26]. A SWNT wrapped by lipids can infiltrate the lipid membrane, as suggested by simulations [22]. Nevertheless, few simulations have been performed on wrapping smaller nanoparticles (such as fullerenes) with lipids and delivering them into a lipid bilayer, though there are already numerous experiments and simulations on the infiltration of bare fullerenes. Although the wrapping lipids seem nontoxic to the lipid bilayer, the effects on the mechanical properties of the biomembranes from using such a nanoparticle delivery method have not yet been illustrated, nor has the efficiency of infiltration with different types of lipids used for wrapping been investigated.

Besides their use in drug delivery and biosensors, nanoparticles can be modified with functional groups on their surface so that the nanoparticles can be functionalized and used for drugs [27–29]. These groups can be connected to nanoparticles by chemical bonds. The study of cellular transport of functionalized gold nanoparticles suggests the value of this method [30]. Fullerenes can be polyhydroxylated for applications in tumor theranostics [31]. They can also be implemented into biosensors, modified by other chemical functional groups [32]. However, this functionalizing process contributes to some changes in the behavior of the nanoparticles within the biomembrane. A polyhydroxylated C_{60} is inclined to attach to the surface of a lipid bilayer though a bare C_{60} prefers to enter the interior of the bilayer and interacts with the biomembrane [33, 34]. Nevertheless, whether the hydroxyl can still change the infiltration behavior if it is coated on nanoparticles of other shapes and sizes, such as SWNTs, has not been completely explored.

To gather more details of this method of delivering nanoparticles by wrapping them with lipids, and to test its feasibility, a series of simulations have been performed in this study. To understand the effects the wrapped or polyhydroxylated nanoparticles have on a biomembrane, in this study we focused on the influence on the lateral diffusivity and lateral strength of the lipid bilayer induced by lipid-wrapping C_{60} and polyhydroxylated SWNTs. We used coarse-grained molecular dynamics simulations offering a time scale and system size at least one order of magnitude larger than available with traditional all-atom molecular dynamics simulations. The diffusion coefficient and scaling factor are adopted to quantify the lipid bilayer diffusivity. The rupture surface tension is used for measurement of the bilayer lateral strength.

2 Methods

The Martini coarse-grained (CG) force field (FF) is employed in the molecular dynamic simulation [35, 36]. The CG nanoparticles C_{15} are models of real C_{60} fullerenes with diameters of 0.72 nm. The interaction site "SC4" is assigned to the CG beads while harmonic bonds with a force constant of 1250 $kJ{\cdot}mol^{-1}{\cdot}nm^{-2}$ connect these beads. Models for dipalmitoyl-glycero-phosphocholine (DPPC) and water are taken from the Martini lipid FF. To build models for dipalmitoyl-glycero-phosphoglycerol (DPPG), lysophosphatidylcholine (LPC), and lysophosphatidylglycerol (LPG), we remove one lipid tail or replace a choline bead with a glycerol bead (at interaction site "P4" in the Martini FF) [37]. The Lennard-Jones (LJ) and Coulomb potentials are cut off at 1.2 nm and shifted to zero from 0.9 to 1.2 nm smoothly. We have constructed three sets of fullerenes wrapped by three kinds of lipids, respectively. The number of wrapping lipids varies but the lipid type remains the same in one set of simulations. A bare nanoparticle C_{15} is wrapped by 6, 9, or 12 lipids in a set. We wrap C_{15} with DPPC, DPPG, LPC, and LPG, respectively, by putting a C_{15} with a certain number of lipids in a water box and simulate for 1 μs to equilibrate the system. All the lipids in the box aggregate around the fullerene after the simulation time. Then, a fullerene wrapped by lipids is placed 3 nm away from a equilibrated DPPC lipid bilayer in a water box. The bilayer consists of 768 DPPC lipids (24×16 in one leaflet of the bilayer). All simulations including lipid-wrapping fullerenes are run until 2 μs.

To obtain the model for polyhydroxylated SWNTs, we generate a 4.58-nm-long (6,6) SWNT including 288 carbon atoms with the TubeGen tool [38]. The SWNT modeling has been presented in other studies as follows [37]: The carbon atoms on the SWNT were replaced by an "SC1" CG bead via a one-to-one mapping whose

mass is reduced to 12 atomic mass units to fit the actual mass. To fit the experimental data, $\varepsilon = 2.7$ is applied to the SWNT–lipid tail (SC1-C1) LJ interaction $\left(xV_{LJ}(r_{ij}) = 4\varepsilon_{ij}\left[\left(\frac{\sigma_{ij}}{r_{ij}}\right)^{12} - \left(\frac{\sigma_{ij}}{r_{ij}}\right)^{6}\right]\right)$ while relatively high force constants are applied to the harmonic potential of the bonds ($V_{bond}(b) = (1/2)K_b(b - b_0)^2$) and angles ($V_{angle}(\theta) = (1/2)K_b(b - b_0)^2$). These force-field constants will lead to a rigid-rod SWNT so that the effects of deformation of the SWNT can be ignored in our simulations. After modeling the SWNTs, we coat one SWNT with 30 hydroxyls symmetrically on its surface using chemical bonds, as shown in Fig. 1. Because the hydroxyl in an octanol is treated as a coarse-grained bead and given an interaction site of "P1" in the Martini FF, the CG bead "SP1" is chosen to represent the hydroxyls in the SWNTs to simulate its polar properties in ring particles. The force constants for bonds and angles between the hydroxyl and a carbon atom are the same as those in the Martini FF. The parameters for the bonded interactions in an SWNT are listed in Table 1. We have constructed three systems, containing zero, one, or two coated SWNTs, respectively. A polyhydroxylated SWNT is initially placed 1 nm parallelly from the surface of a equilibrated DPPC bilayer to study the effects of a polyhydroxylated SWNT on the lipid bilayer. When the simulation involves more than one hydroxylated SWNT, the initial distance between two hydroxylated SWNTs is about 3 nm.

The lateral strength of the DPPC bilayer affected by the polyhydroxylated SWNTs is investigated by measuring the rupture pressure of the bilayers. As in our previous work, a constant semi-isotropic pressure coupling is applied on the bilayer system in one simulation [16].

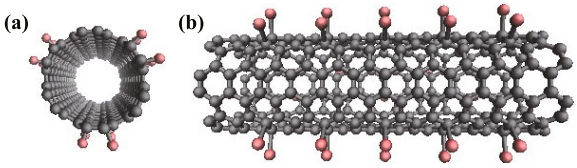

Fig. 1 Structure of a polyhydroxylated SWNT. Black and red represent the carbon atoms and the hydroxyl groups, respectively. The lines in the figure represent the chemical bonds between atoms. **(a)** Front view of a polyhydroxylated SWNT. **(b)** Side view of a polyhydroxylated SWNT.

Table 1 Parameters for the bonded interaction in polyhydroxylated SWNTs.

	Bond		Angle	
	b_0/nm	k_b/(kJ·mol^{-1}·nm^{-2})	θ_0/(°)	k_θ/(kJ·mol^{-1})
Carbon-carbon	0.142	20 000	120	1500
Carbon-hydroxy	0.143	1250	110	25

Initially, the system is coupled to high pressure close to the threshold for rupture (−60 to −120 bar, depending on the size of the simulation box) and it becomes equilibrated. Then, the system is coupled to higher pressure, and this leads to breakage of the bilayer. In this way, the critical rupture tension is measured. To estimate the lateral strength, the surface tension is computed from the average surface tension:

$$R = L_z(P_N - P_L), \tag{1}$$

where R is the surface tension, L_z is the thickness of the bilayer, and P_N and P_L are the normal component and lateral components, respectively, of the pressure tensor.

Gromacs software, Version 4.6.3, is used for all simulations [39, 40]. A constant temperature of 320 K is applied in all simulations using the Berendsen scheme [41]. Periodic boundary conditions are used in all simulations. The coupling constant is 0.2 ps for pressure coupling and 0.1 ps for temperature. The time step of the simulations is 40 fs, except for those including polyhydroxylated SWNTs, for which we use 8 fs. All systems are duplicated at least three times.

3 Results and discussion

The mixture of C_{60} and wrapping lipids is sphere-like with the lipid heads pointing outward and the C_{60} being almost in the core of this mixture. The initial placements of the mixtures away from the bilayer are the same. After 1 μs, the mixture of C_{60} and wrapping lipids DPPC, LPC, and LPG enter one leaflet of the DPPC bilayer as a whole. Then, the wrapping lipids around the C_{60} drop off from the C_{60} after infiltration. These lipids mix with the original DPPC lipids in the bilayer and diffuse through the membrane. The process of insertion is shown in Fig. 2. However, the insertion of C_{60} wrapped by DPPG is not observed in the simulations, as is similar to the results of DPPG wrapping SWNTs [22]. A bare C_{60} enters the DPPC bilayer in our simulation, as has been indicated by other simulations and experiments [14, 42]. In the simulations of polyhydroxylated SWNTs, the polyhydroxylated SWNT attaches onto the surface of the DPPC bilayer and it is later half buried beneath the surface with a side of the coated SWNT exposed to the water, as shown in Fig. 3, unlike the insertion of a bare SWNT in which one end of the SWNT inserts into the bilayer first and finally the entire SWNT stays in the center of the bilayer [22]. In previous experiments [33], the results suggest that the polyhydroxylated C_{60} prefers to attach onto the surface of the bilayer rather than getting into the interior of the biomembrane, which

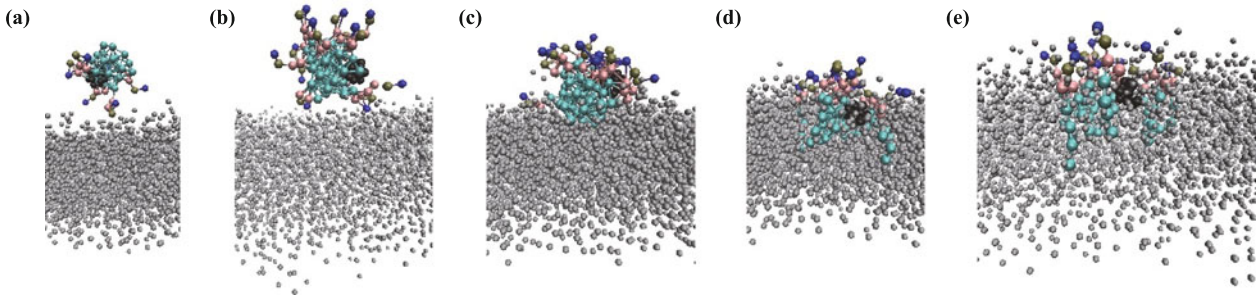

Fig. 2 **(a)** Snapshot of the system before the fullerene wrapped by LPC lipids inserts into the DPPC lipid bilayer. Blue, brown, pink, and cyan represent the choline, phosphate, glycerol, and lipid tail of the LPC lipids while black represents the coarse-grained beads of the carbon atoms in C_{60}. Water is omitted. For clarity, the DPPC lipid molecules are represented in gray. **(b)** The mixture of fullerene and LPC lipids begins to touch the surface of the lipid bilayer. **(c)** At the beginning of the insertion, the mixture enters one leaflet of the bilayer as a whole. **(d)** As the mixture enters the bilayer, the LPC lipids began to drop off the fullerene with their lipid heads pointing toward the water environment. **(e)** After the insertion, the LPC lipids drop off the fullerene completely and they diffuse into the lipid bilayer. The fullerene stays in the interior of the lipid bilayer.

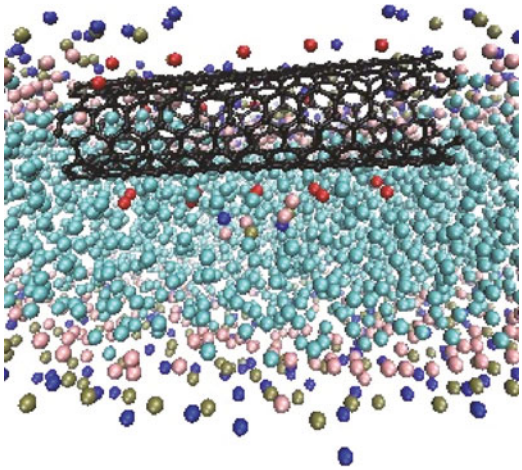

Fig. 3 Final position of the polyhydroxylated SWNT after its insertion into the DPPC bilayer. Blue, brown, pink, cyan, black, and red represent the choline, phosphate, glycerol, lipid tail, and carbon atoms of the polyhydroxylated SWNT hydroxyl, respectively. The lines in the figure represent the chemical bonds between carbon atoms. After the insertion, the polyhydroxylated SWNT does not get into the interior of the lipid bilayer. It is beneath the membrane's surface, and part of the polyhydroxylated surface is exposed to the water. For clarity, water is omitted.

is similar to our results obtained from simulations on polyhydroxylated SWNTs, though they are different in geometry. **(e)** After the insertion, the LPC lipids drop off the fullerene completely and they diffuse in the lipid bilayer. The fullerene stays in the interior of the lipid bilayer.

The molecules or functional groups around the surface of the nanoparticles can greatly affect the nanoparticle insertion process and the final state of the nanoparticles inside the biomembrane. The observation that a bare C_{60} inserts into the DPPC while the one wrapped by DPPG does not might be attributed to interaction between the wrapping DPPGs and the DPPC bilayer. The hydroxyls coated on the SWNTs make the SWNTs attach onto the membrane surface initially and prevent it from going inside to the center of the bilayer, which is suggested by experiments with polyhydroxylated fullerenes [33].

To characterize the effects of C_{60} wrapped by lipids or polyhydroxylated SWNTs on the diffusivity of the lipid bilayer after the nanoparticles get inside the bilayer, the lateral diffusion coefficient and lateral scaling factor of the DPPC bilayer are calculated. As the lipid-wrapping C_{60} and the polyhydroxylated SWNT infiltrate only one leaflet of the DPPC bilayer, the diffusion coefficients and lateral scaling factors are averaged through this leaflet. The diffusion behavior of a lipid in a bilayer satisfies the scaling law

$$L(t) \sim t^k, \tag{2}$$

where $L(t)$ is the root-mean-square displacement of a lipid molecule, t represents time, and k is the scaling factor. The calculated diffusion coefficient and scaling factor are averaged over all the DPPC lipids within the bilayer in 1 μs. The calculation does not consider the contribution of the wrapping lipids that enter the membrane later.

The rupture surface tension is also computed to quantify the lateral strength of the DPPC bilayer affected by the wrapped C_{60} and polyhydroxylated SWNTs. Because previous work on rupture tension has already shown that the fullerenes C_{60} could strengthen the membrane lateral strength [16], only the rupture tension of the lipid bilayer affected by hydroxylated SWNTs is computed.

3.1 Effects of the wrapped or coated nanoparticles on the lipid bilayer diffusivity

3.1.1 Lateral diffusion coefficient is computed when the lipid bilayer is equilibrated

The lateral diffusion coefficient of the DPPC bilayer is

Table 2 Diffusion coefficients and scaling factors of the DPPC bilayer when the system is equilibrated after the insertion of different types of nanoparticles.

Type of nanoparticles	None[1)]	Bare fullerene[2)]	6DPPC[3)]	6LPC	6LPG	12DPPC	12LPC	12LPG	1SWNT[4)]	2SWNTs
Diffusion coefficient/ $(10^{-5}\mathrm{cm}^2\cdot\mathrm{s}^{-1})$	0.0751	0.0701	0.0712	0.0770	0.0722	0.0729	0.0725	0.0794	0.0629	0.0690
Scaling factor	0.50801	0.48508	0.47703	0.47706	0.51065	0.48295	0.45951	0.48573	0.46955	0.49210

1) "None" represents the controlled group without nanoparticles insertions.
2) "Bare fullerene" stands for the samples with a bare C_{60} insertion.
3) The effects induced by 6 DPPCs wrapping C_{60} is illustrated in "6DPPC" and the other samples are represented in a similar way.
4) The diffusion coefficient of the lipid bilayer inserted by one polyhydroxylated SWNTs is represented in "1SWNT" and the result for two polyhydroxylated is illustrated in the same way.

computed and the results are listed in Table 2 when the system is equilibrated after the insertion of the nanoparticles. The lateral diffusion coefficient is averaged from 1 to 2 μs after the insertion, which took place at 0 μs. Compared with the data averaged from 2 to 6 μs, the data show that the system is well equilibrated at 2 μs. The data from 2 to 6 μs are shown in the inserted figure of Fig. 4. The ratio of C_{60} to lipids within the bilayer is 1:768 after the wrapped C_{60} insertion. A controlled sample of a DPPC bilayer without any nanoparticles insertion is used for contrast.

The membrane affected by wrapped or coated nanoparticles has a lower diffusivity, except those inserted with C_{60} wrapped by either 12 LPGs or 6 LPCs. A bare C_{60} without wrapping leads to a smaller bilayer diffusion coefficient than the controlled group, which corresponds to the results obtained from previous work [16]. The diffusion coefficient of the controlled group in which only a DPPC bilayer is in the water box also corresponds to the reported results [16, 36]. The C_{60} wrapped by 12 LPGs and those wrapped by 6 LPCs increase the diffusion coefficient at 5.73% and 2.52%, respectively, compared with a DPPC bilayer of the same structure without nanoparticle insertion. The polyhydroxylated SWNTs hinder the diffusivity of the membrane. The mixture of lipid bilayer and one polyhydroxylated SWNT has 19.4% lower diffusivity than the controlled bilayer. Nevertheless, one single polyhydroxylated SWNT causes larger decrease in the biomembrane diffusivity than two polyhydroxylated SWNTs. The smaller diffusion coefficient of the polyhydroxylated SWNT–bilayer mixture is suggested by research on a CNT-embedded lipid bilayer, in which the bare CNTs hinder the diffusion of the bilayer [43]. This result demonstrates that the polyhydroxylated SWNT hampers the diffusion of the lipid molecule in the bilayer like a bare SWNT.

To characterize the effects of the wrapping lipids on the diffusivity of the DPPC lipid bilayer, samples containing only12 wrapping lipids inserting without C_{60} into the bilayer are studied. When the system is equilibrated, the diffusion coefficient has increased 16.2%, led by 12 wrapping LPCs, while the 12 wrapping LPGs have little effect on the diffusivity. The diffusion coefficients of the lipid bilayer inserted by 12 wrapping DPPCs approximates the controlled bilayer as expected for they are of the same type of lipid. The ratio of the inserting wrapping lipids to the original lipids in the DPPC bilayer $< 1.7\%$. The results suggest that wrapping lipids of different type may cause an increase in the extent of DPPC bilayer diffusivity. It also suggests that a mixture of different types of bilayer lipids and wrapping lipids may contribute to a change in the bilayer diffusion coefficient after the system is equilibrated, even though the ratio of the inserted lipids to the initial bilayer lipid is low. This corresponds to the result that bilayers built up by different types of lipids may have different diffusion coefficients [44]. It also suggested that the diffusion coefficient of the bilayer system can be changed by mixing the bilayer with other types of lipids [44]. This result might explain the extraordinary increase in the bilayer's diffusivity induced by the 12 LPGs and 6 LPCs wrapping fullerenes, though a bare C_{60} reduces it. The results of the diffusion coefficient affected by wrapping lipids are listed in Table 3.

The changes in diffusion coefficients show that a bare C_{60} insertion induces a decline in bilayer diffusivity while

Table 3 Diffusion coefficients and scaling factors of the DPPC bilayer affected by the wrapping lipids. [1)]

Type of nanoparticles	Bare fullerene[2)]	None[3)]	12DPPC[4)]	12LPC	12LPG
Diffusion coefficient/$(10^{-5}\mathrm{cm}^2\cdot\mathrm{s}^{-1})$	0.0701	0.0751	0.0737	0.0873	0.0753
Scaling factor	0.48508	0.50801	0.51829	0.51354	0.50407

1) C_{60} is removed from the system and the wrapping lipids insert the bilayer in the simulations.
2) "Bare fullerene" stands for the samples with a bare C_{60} insertion. It is presented for comparisons.
3) "None" represents the controlled group without any nanoparticle insertion.
4) The effects of the 12 wrapping LPCs on the biomembrane is represented in "12 LPC" and the others are in a similar way.

the insertion with wrapping lipids leads to an increase of diffusion coefficient. While the bare C_{60} and wrapping lipids combine together and become a wrapped nanoparticle, a decline of diffusivity is observed in most of the samples except for the 12 LPGs and 6 LPCs wrapping C_{60}.

3.1.2 Evolution of the lateral diffusion coefficient is observed before the bilayer is equilibrated

After the wrapped nanoparticles insert into the lipid bilayer, the diffusion coefficient will experience a rise before it returns to the value when the system was is equilibrium, no matter whether the latter is larger or smaller than the diffusion coefficient before insertion. To illustrate this phenomenon, the diffusion coefficient averaged from 0 to 1 μs is computed and it is compared with that averaged from 1 to 2 μs. The time evolution of the diffusion coefficient induced by C_{60} wrapped by different types of lipids is shown in Fig. 4. At 2 μs, the system is considered to be equilibrated.

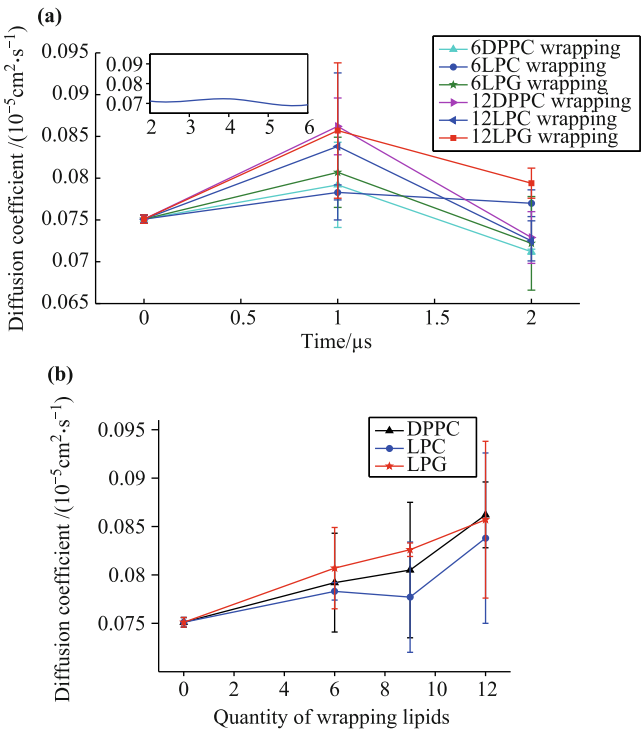

Fig. 4 **(a)** Evolution of the diffusion coefficient after the nanoparticles wrapped by lipids insert into the biomembrane. The diffusion coefficient rises and then falls to the value when the system becomes equilibrated. At time 0 μs, the nanoparticles insert into the lipid bilayer. The behavior of the diffusion coefficient after 2 μs is shown in the inserted figure. The diffusion coefficient changes little after 2 μs, which suggests that the system has equilibrated in 2 μs. **(b)** Relation between the quantity of wrapping lipids and the diffusion coefficient averaged from 0 to 1 μs before the system becomes equilibrated. The ratio of C_{60} to lipids within the bilayer is 1:768 after the wrapped C_{60} insertion. The diffusion coefficient increases as the quantity of wrapping lipids grows except that the diffusion coefficient affected by 9 LPCs wrapping C_{60} is lower than that by 6 LPCs wrapping C_{60}.

This increase of diffusivity before the system reaches equilibrium has a regular pattern that is positively correlated with the number of wrapping lipids around C_{60}, except that 6 LPCs wrapping fullerenes leads to higher diffusivity than 9 LPCs wrapping fullerenes. This pattern is shown in Fig. 4. The data in Fig. 4 are averaged from 1 to 2 μs, before the system is equilibrated. Considering the samples wrapped by LPCs, we see that the diffusion coefficient of the biomembrane has increased 7.02% as the ratio of inserting LPC lipids to the original DPPC lipids in the bilayer increases from 0.78% to 1.56%. For a certain type of wrapping lipid, as the quantity of the wrapping lipids increases, the diffusivity of the lipid bilayer 1 μs right after the insertion took place is enhanced. The enhancement is also related to the type of wrapping lipid. For the same number of wrapping lipids, the increase of diffusivity of the bilayer induced by DPPCs or LPGs is greater than that by LPGs.

Interestingly, the wrapping DPPCs can also result in an enhancement in diffusivity 1 μs after the infiltration even though they are of the same kind as the lipids building up the bilayer. Especially, the increment of diffusivity in 1 μs rises as the quantity of the wrapping DPPCs increases. This phenomenon suggests that the enhancement of the diffusivity before equilibrium may not be only attributed to the effects of the mixture between different sorts of lipids but may also result from some other factors, such as the size of the wrapped nanoparticles. Though the size effect on the diffusivity of biomembranes by lipid-wrapping nanoparticles was not illustrated in previous research, the size of bare carbon nanoparticles affecting diffusivity has been investigated, which might support our inference [16].

The results have shown that the bilayer diffusivity is affected by the wrapped nanoparticles regardless of whether the system is equilibrated. The diffusivity is changed by the wrapped nanoparticles before equilibrium. This change has a regular pattern related to the quantity and type of wrapping lipids. When the system is equilibrated, the wrapped nanoparticles also cause a change in the diffusivity of the DPPC bilayer because the wrapped C_{60} decreases the bilayer diffusion coefficient while the wrapping lipids enhance it. The changes of diffusivity after 2 μs might be attributed to the interaction between different types of lipids or to the interactions between C_{60} and lipids, while the changes at 1 μs might be related to the total size of the inserting nanoparticle wrapped by lipids.

3.1.3 Scaling factor is computed when the lipid bilayer is equilibrated

However, unlike the obvious and regular variation in diffusion coefficient, only a slight and irregular change of the scaling factor of the DPPC bilayer is observed, as demonstrated in Table 2. A controlled bilayer that is not affected by nanoparticles has a scaling factor $\sim 1.58\%$ larger than 0.5. The insertion of bare C_{60} and hydroxyl-coated SWNTs causes a slight reduction in the scaling factor but is no larger than 10% compared with the controlled bilayer. The scaling factors of the bilayers influenced by wrapped C_{60} or polyhydroxylated SWNTs remain ≈ 0.5. The data are presented in Table 2.

To investigate whether the wrapping lipids have little effect on bilayer diffusion, the scaling factors of samples that include only wrapping lipid insertion without C_{60} are computed. The results are listed in Table 3. The scaling factors stay at ~ 0.5, and no more than 2% variation is observed. This illustrates that the DPPC bilayer remains in approximate free diffusion after the wrapping lipids infiltrated.

All the samples exhibit a slight change in the scaling factor though some of them have huge distinctions in diffusion coefficient. The scaling factor approximates 0.5 in all the samples, which suggests that the diffusion patterns remain free. However, the scaling factor is not always 0.5 in crowded systems. Our simulations show that the lipid bilayer remains in free diffusion when the ratio of the C_{60} to the lipids in the membrane is $<1{:}768$. Nonetheless, the approximation of the scaling factors before and after the nanoparticle insertions still suggests that these nanoparticles have only a slight influence on the diffusion pattern.

3.1.4 Scaling factor is computed before the lipid bilayer is equilibrated

The scaling factor of the DPPC bilayer before the system is equilibrated is computed to contrast the enhancement of the diffusion coefficient averaged from 0 to 1 μs. As shown in Fig. 5, the scaling factor is ~ 0.5 in 1 μs and changes little, although the diffusion coefficient rises before the system is equilibrated. No regular pattern of scaling factor change is observed as the number of wrapping lipids increase. The quantity and type of wrapping lipid may have a slight influence on the scaling factor before the system is equilibrated. The scaling factor for LPC wrapping is lower than those of DPPC or LPG wrapping, but the difference of the scaling factor in 1 μs between LPC wrapping and the controlled sample is $<10\%$.

The scaling factors before or after equilibrium are ≈ 0.5

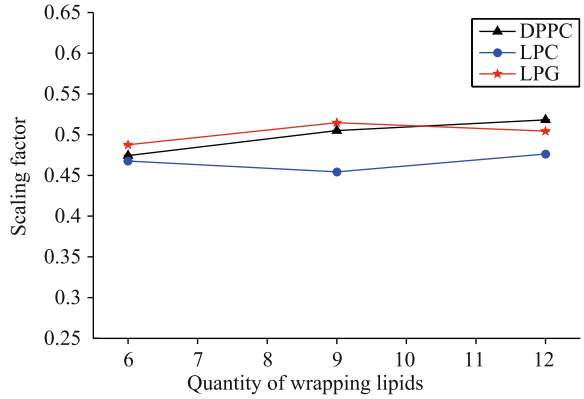

Fig. 5 Scaling factor of the DPPC bilayer averaged from 0 to 1 μs before the system is equilibrated. The scaling factor is slightly changed after the wrapping fullerene insertions, especially in the samples that contain LPCs wrapping C_{60}. However, the scaling factor is still near 0.5. There is no regular change of the scaling factor as the quantity of the wrapping lipids grows. The results suggest that the insertion of the lipid-wrapping C_{60} has little effect on the diffusion pattern of the biomembrane, regardless of whether the membrane is equilibrated.

after the insertion of wrapped nanoparticles. It can be seen from this result that the diffusion mechanism of the DPPC bilayer is only slightly changed. Given the nature of the diffusion, the equilibrated diffusion behavior might be similar to that before equilibrium.

There is only a slight change of the scaling factor when the system evolves into equilibrium, while the diffusion coefficient has experienced an increase and finally returns to its equilibrated value. The scaling factor is near 0.5 all the time while the diffusion coefficient changes as the quantity and type of wrapping lipids vary. The diffusion coefficient is also influenced by the polyhydroxylated SWNTs. This suggests that the extent of diffusivity of a membrane can be affected by the wrapped nanoparticles, wrapping lipids, and coating molecules, whereas the change in the diffusivity pattern is very slight because the scaling factor is always near 0.5, which indicates that the diffusion pattern is very similar to free diffusion.

The infiltration process of the wrapped C_{60} and its slight effects on the diffusivity mechanism of the lipid bilayer serve as a test of the feasibility of delivering nanoparticles with certain types of lipids. Our simulations suggest that the diffusivity patterns of the biomembranes are not changed, regardless of the type of lipid. To deliver a specific nanoparticle into a DPPC bilayer, if we want to maintain the influence on the bilayer by this wrapped nanoparticle, the DPPC lipid should be chosen for wrapping. If we hope the extent of diffusivity to remain steady after the infiltration of a fullerene such as C_{60}, we can wrap the fullerene with LPCs to increase the diffusivity of the bilayer when they are mixed with the DPPCs and compensate for the decline induced by

the fullerenes. However, wrapping the nanoparticles with DPPGs might lead to delivery failure as the insertions of fullerenes wrapped by DPPGs are not observed in the simulations.

3.2 Effects of nanoparticles on biomembrane rupture tension

The rupture tension can be affected by nanoparticles either wrapped by lipids or coated by hydroxyls. To explore the effects of polyhydroxylated SWNTs on a lipid bilayer, the critical tension at the instant that the irreversible pore forms is measured to quantify the strength of the bilayer. The rupture tension is shown in Fig. 6.

The rupture tension varies as the quantity of the polyhydroxylated SWNTs increases. The rupture tension of the controlled sample, which contains only a DPPC bilayer without polyhydroxylated SWNTs, is about 64 mN/m. This result is consistent with previous work in which the rupture tension of DPPC bilayers was measured [16]. When one polyhydroxylated SWNT is added to the system, the rupture tension has decreased by 5.05%. Nevertheless, when one more polyhydroxylated SWNT is added to the system, the rupture tension has increased by 13.40% compared to that of the controlled DPPC bilayer. When two polyhydroxylated SWNTs affect the lipid bilayer, the rupture tension increases by 19.43% compared with that when the system contains only one polyhydroxylated SWNT. This variation suggests that the hydroxyl-coated SWNT will affect the strength of the biomembrane. When only one polyhydroxylated SWNT is buried beneath the surface of the membrane, the strength of the lipid bilayer is weakened. When two coated SWNTs are within the membrane, the lateral strength is enhanced.

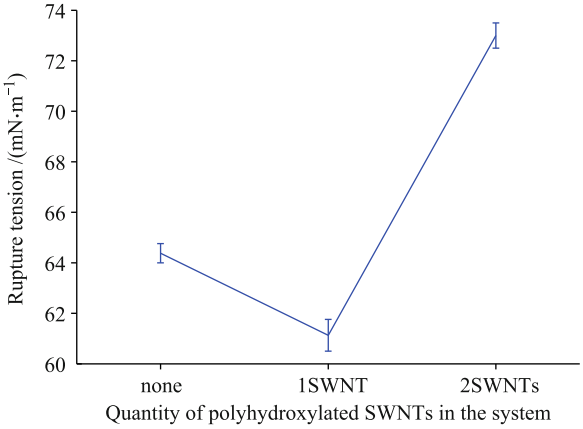

Fig. 6 Rupture tension of the lipid bilayer infiltrated by polyhydroxylated SWNTs. The controlled group, which only contains a DPPC bilayer in a water box, is represented by "none." When one polyhydroxylated SWNT infiltrates the bilayer, the rupture tension after this insertion is shown by "1SWNT" and the result for two polyhydroxylated SWNTs is represented in a similar way. The rupture tension of the DPPC bilayer is reduced if one polyhydroxylated SWNT is inserted. However, when two polyhydroxylated SWNTs are added to the system, the tension is increased, compared with that of the controlled group.

4 Conclusion

We have discussed the influences on the diffusivity and lateral strength of a lipid bilayer induced by lipid-wrapping C_{60} and polyhydroxylated SWNTs. The results are obtained by using coarse-grained molecular dynamics and they are contrasted with each other and other studies to reach our conclusions.

Lipid-wrapping C_{60} can infiltrate the lipid bilayer, except those wrapped by DPPGs, and the C_{60} stays in the interior while the wrapping lipids shed from the C_{60} and diffuse within the bilayer like other lipids that make up the membrane. The polyhydroxylated SWNT is buried beneath the surface of the bilayer, unlike a bare SWNT. The lipid bilayer remains in free diffusion after the infiltration of the lipid-wrapping C_{60} or hydroxylated SWNTs while these nanoparticles can change the extent of the diffusivity. Before equilibrium, this change is related to the quantity and type of wrapping lipids. After the system is equilibrated, there is still an obvious change in the diffusion coefficient but the scaling factor changes only slightly, suggesting that the lipid-wrapping C_{60} affects the extent of the bilayer's diffusivity but that the diffusion pattern of the lipid bilayer remains approximately free. These results serve to test the feasibility of delivering lipid-wrapping nanoparticles into biomembranes. Some suggestions for choosing appropriate lipids for wrapping are given.

The lateral strength of the lipid bilayer is affected by polyhydroxylated SWNTs. In our observation, the rupture tension of the biomembrane is not linearly related to the quantity of polyhydroxylated SWNTs inserted into the bilayer. The lateral strength of the biomembrane can be either increased or decreased by the polyhydroxylated SWNTs, depending on their quantity.

Our studies have demonstrated the influence on the mechanical properties of the lipid bilayer by lipid-wrapping nanoparticles and hydroxylated nanoparticles. These results might be of help in the application of drug delivery, enabling the choice of the proper lipid to use for the drug envelope and helping us understanding the effects induced by such envelopes. They also provide some insight into intentionally changing the lateral strength of biomembranes, a method that could be implemented in biomembrane synthesis.

Acknowledgements The authors acknowledge financial support from the National Nature Foundation of China (NSFC Nos. 11004255 and 11004256).

References

1. M. E. Samberg, S. J. Oldenburg, and N. A. Monteiro-Riviere, Evaluation of silver nanoparticle toxicity in skin in vivo and keratinocytes in vitro, *Environ. Health Perspect.* 118(3), 407 (2010)
2. B. J. Marquis, S. A. Love, K. L. Braun, and C. L. Haynes, Analytical methods to assess nanoparticle toxicity, *Analyst* 134(3), 425 (2009)
3. X. Yang, A. P. Gondikas, S. M. Marinakos, M. Auffan, J. Liu, H. Hsu-Kim, and J. N. Meyer, Mechanism of silver nanoparticle toxicity is dependent on dissolved silver and surface coating in *caenorhabditis elegans*, *Environ. Sci. Technol.* 46(2), 1119 (2012)
4. M. Schulz, A. Olubummo, and W. H. Binder, Beyond the lipid-bilayer: Interaction of polymers and nanoparticles with membranes, *Soft Matter* 8(18), 4849 (2012)
5. A. A. Skandani, R. Zeineldin, and M. Al-Haik, Effect of chirality and length on the penetrability of single-walled carbon nanotubes into lipid bilayer cell membranes, *Langmuir* 28(20), 7872 (2012)
6. Y. I. Prylutskyy, V. M. Yashchuk, K. M. Kushnir, A. A. Golub, V. A. Kudrenko, S. V. Prylutska, I. I. Grynyuk, E. V. Buzaneva, P. Scharff, T. Braun, and O. P. Matyshevska, Biophysical studies of fullerene-based composite for bio-nanotechnology, *Mater. Sci. Eng. C* 23(1-2), 109 (2003)
7. N. A. Kouklin, W. E. Kim, A. D. Lazareck, and J. M. Xu, Carbon nanotube probes for single-cell experimentation and assays, *Appl. Phys. Lett.* 87(17), 173901 (2005)
8. S. D. Caruthers, S. A. Wickline, and G. M. Lanza, Nanotechnological applications in medicine, *Curr. Opin. Biotechnol.* 18(1), 26 (2007)
9. L. Zhang, F. X. Gu, J. M. Chan, A. Z. Wang, R. S. Langer, and O. C. Farokhzad, Nanoparticles in medicine: therapeutic applications and developments, *Clin. Pharmacol. Ther.* 83(5), 761 (2008)
10. D. A. Groneberg, M. Giersig, T. Welte, and U. Pison, Nanoparticle-based diagnosis and therapy, *Curr. Drug Targets* 7(6), 643 (2006)
11. P. Mroz, A. Pawlak, M. Satti, H. Lee, T. Wharton, H. Gali, T. Sarna, and M. R. Hamblin, Functionalized fullerenes mediate photodynamic killing of cancer cells: Type I versus Type II photochemical mechanism, *Free Radic. Biol. Med.* 43(5), 711 (2007)
12. J. Lin, H. Zhang, Z. Chen, and Y. Zheng, Penetration of lipid membranes by gold nanoparticles: insights into cellular uptake, cytotoxicity, and their relationship, *ACS Nano* 4(9), 5421 (2010)
13. Y. Li, X. Chen, and N. Gu, Computational investigation of interaction between nanoparticles and membranes: Hydrophobic/hydrophilic effect, *J. Phys. Chem. B* 112(51), 16647 (2008)
14. J. Wong-Ekkabut, S. Baoukina, W. Triampo, I. M. Tang, D. P. Tieleman, and L. Monticelli, Computer simulation study of fullerene translocation through lipid membranes, *Nat. Nanotechnol.* 3(6), 363 (2008)
15. K. Yang and Y. Q. Ma, Computer simulation of the translocation of nanoparticles with different shapes across a lipid bilayer, *Nat. Nanotechnol.* 5(8), 579 (2010)
16. K. Lai, B. Wang, Y. Zhang, and Y. Zheng, Computer simulation study of nanoparticle interaction with a lipid membrane under mechanical stress, *Phys. Chem. Chem. Phys.* 15(1), 270 (2013)
17. X. Zhang, Y. Zhang, Y. Zheng, and B. Wang, Mechanical characteristics of human red blood cell membrane change due to C_{60} nanoparticle infiltration, *Phys. Chem. Chem. Phys.* 15(7), 2473 (2013)
18. J. Kolosnjaj, H. Szwarc, and F. Moussa, Bio-Applications of Nanoparticles, Springer, 2007, page 168
19. C. A. Poland, R. Duffin, I. Kinloch, A. Maynard, W. A. Wallace, A. Seaton, V. Stone, S. Brown, W. Macnee, and K. Donaldson, Carbon nanotubes introduced into the abdominal cavity of mice show asbestos-like pathogenicity in a pilot study, *Nat. Nanotechnol.* 3(7), 423 (2008)
20. T. Xia, M. Kovochich, J. Brant, M. Hotze, J. Sempf, T. Oberley, C. Sioutas, J. I. Yeh, M. R. Wiesner, and A. E. Nel, Comparison of the abilities of ambient and manufactured nanoparticles to induce cellular toxicity according to an oxidative stress paradigm, *Nano Lett.* 6(8), 1794 (2006)
21. G. Jia, H. Wang, L. Yan, X. Wang, R. Pei, T. Yan, Y. Zhao, and X. Guo, Cytotoxicity of carbon nanomaterials: Single-wall nanotube, multi-wall nanotube, and fullerene, *Environ. Sci. Technol.* 39(5), 1378 (2005)
22. H. Lee, Interparticle dispersion, membrane curvature, and penetration induced by single-walled carbon nanotubes wrapped with lipids and PEGylated lipids, *J. Phys. Chem. B* 117(5), 1337 (2013)
23. A. Z. Wang, R. Langer, and O. C. Farokhzad, Nanoparticle delivery of cancer drugs, *Annu. Rev. Med.* 63(1), 185 (2012)
24. A. Babu, A. K. Templeton, A. Munshi and R. Ramesh, Nanoparticle-based drug delivery for therapy of lung cancer: progress and challenges, *Journal of Nanomaterials*, 2013 (2013)
25. D. Pozzi, C. Marchini, F. Cardarelli, A. Rossetta, V. Colapicchioni, A. Amici, M. Montani, S. Motta, P. Brocca, L. Cantù, and G. Caracciolo, Mechanistic understanding of gene delivery mediated by highly efficient multicomponent envelope-type nanoparticle systems, *Mol. Pharm.* 10(12), 4654 (2013)
26. S. Tan, X. Li, Y. Guo, and Z. Zhang, Lipid-enveloped hybrid nanoparticles for drug delivery, *Nanoscale* 5(3), 860 (2013)
27. P. Majewski and B. Thierry, Functionalized magnetite nanoparticles - synthesis, properties, and bio-applications, *Crit. Rev. Solid State Mater. Sci.* 32(3), 203 (2007)

28. S. G. Grancharov, H. Zeng, S. Sun, S. X. Wang, S. O'Brien, C. B. Murray, J. R. Kirtley, and G. A. Held, Bio-functionalization of monodisperse magnetic nanoparticles and their use as biomolecular labels in a magnetic tunnel junction based sensor, *J. Phys. Chem. B* 109(26), 13030 (2005)
29. S. Yu, and G. M. Chow, Carboxyl group (-CO2H) functionalized ferrimagnetic iron oxide nanoparticles for potential bio-applications, *J. Mater. Chem.* 14(18), 2781 (2004)
30. J. D. Peters, Cellular Transport of Functionalized Gold Nanoparticles, Ph. D. Thesis, Worcester: Worcester Polytechnic Institute, 2013
31. Z. Chen, L. Ma, Y. Liu, and C. Chen, Applications of functionalized fullerenes in tumor theranostics., *Theranostics* 2(3), 238 (2012)
32. W. Hong, H. Bai, Y. Xu, Z. Yao, Z. Gu, and G. Shi, Preparation of gold nanoparticle/graphene composites with controlled weight contents and their application in biosensors, *J. Phys. Chem. C* 114(4), 1822 (2010)
33. J. Grebowski, A. Krokosz and M. Puchala, Membrane fluidity and activity of membrane ATPases in human erythrocytes under the influence of polyhydroxylated fullerene, *Biochimica et Biophysica Acta (BBA)-Biomembranes* 1828, 241 (2012)
34. D. Baowan, B. J. Cox, and J. M. Hill, Instability of C_{60} fullerene interacting with lipid bilayer, *J. Mol. Model.* 18(2), 549 (2012)
35. S. J. Marrink, H. J. Risselada, S. Yefimov, D. P. Tieleman, and A. H. de Vries, The MARTINI force field: coarse grained model for biomolecular simulations, *J. Phys. Chem. B* 111(27), 7812 (2007)
36. S. J. Marrink, A. H. de Vries, and A. E. Mark, Coarse grained model for semiquantitative lipid simulations, *J. Phys. Chem. B* 108(2), 750 (2004)
37. H. Lee and H. Kim, Self-assembly of lipids and single-walled carbon nanotubes: Effects of lipid structure and PEGylation, *J. Phys. Chem. C* 116(16), 9327 (2012)
38. TubeGen 3.4 (web-interface, http://turin.nss.udel.edu/research/tubegenonline.html), J. T. Frey and D. J. Doren, University of Delaware, Newark DE, 2011
39. H. J. C. Berendsen, D. van der Spoel, and R. van Drunen, GROMACS: A message-passing parallel molecular dynamics implementation, *Comput. Phys. Commun.* 91(1-3), 43 (1995)
40. E. Lindahl, B. Hess and D. Van Der Spoel, GROMACS 3.0: A package for molecular simulation and trajectory analysis Molecular modeling annual 7, 306 (2001)
41. H. J.C. Berendsen, J. P. M. Postma, W. F. van Gunsteren, A. DiNola, and J.R. Haak, Molecular dynamics with coupling to an external bath, *J. Chem. Phys.* 81(8), 3684 (1984)
42. R. Qiao, A. P. Roberts, A. S. Mount, S. J. Klaine, and P. C. Ke, Translocation of C_{60} and its derivatives across a lipid bilayer, *Nano Lett.* 7(3), 614 (2007)
43. X. Li, Y. Shi, B. Miao, and Y. Zhao, Effects of embedded carbon nanotube on properties of biomembrane, *J. Phys. Chem. B* 116(18), 5391 (2012)
44. R. Abedi Karjiban, N. S. Shaari, U. V. Gunasakaran and M. Basri, A Coarse-Grained Molecular Dynamics Study of DLPC, DMPC, DPPC, and DSPC Mixtures in Aqueous Solution, *Journal of Chemistry*, 2013 (2013)